Fluorination induced half metallicity in two-dimensional few zinc oxide layers

Qian Chen,[1] Jinlan Wang,[1,2,a)] Liyan Zhu,[1] Shudong Wang,[1] and Feng Ding[3]
[1]*Department of Physics, Southeast University, Nanjing 211189, People's Republic of China*
[2]*School of Chemistry and Chemical Engineering, Southeast University, Nanjing 211189, China*
[3]*Institute of Textiles and Clothing, Hong Kong Polytechnic University, Kowloon, Hong Kong*

(Received 2 April 2010; accepted 12 May 2010; published online 27 May 2010)

We systematically explore the stability, bonding characteristics, and electronic and magnetic properties of two-dimensional (2D) few zinc oxide layers (few-ZnOLs) with or without fluorination by using density functional theory approach. The pristine few-ZnOLs favor stable planar hexagonal structures, which stem from their unique bonding characteristics: The intralayer Zn–O interaction is dominated by covalent bonding while the interaction between layers is weak ionic bonding. Furthermore, we demonstrate that fluorination from one side turns the planar few-ZnOLs back to the wurtzitelike corrugated structure, which enhances the stability of the 2D ZnO films. The fluorinated few-ZnOLs are ferromagnets with magnetic moments as high as 0.84, 0.87, 0.89, and 0.72 μ_B per unit cell for the number of layers of N=1, 2, 3, and 4, respectively. Most interestingly, the fluorination can also turn few-ZnOLs from semiconductor into half metallicity with a half-metal gap up to 0.56 eV. These excellent electronic and magnetic properties may open 2D ZnO based materials great opportunity in future spintronics. © *2010 American Institute of Physics*.
[doi:10.1063/1.3442908]

I. INTRODUCTION

Graphene, a single atomic layer thick two-dimensional (2D) material, has been extensively investigated both experimentally and theoretically because of its unique mechanical, electronic, and magnetic properties.[1–3] However a perfect graphene owns almost zero band gap, which prevents it to be an ideal semiconducting material for electronic application, in which a medium band gap as that of silicon (~0.7 eV) is required.

Beyond nanocarbon, zinc oxide (ZnO) is probably the mostly studied nanomaterial because of its diverse applications in chemical sensing, high transparency, piezoelectricity, biocompatibility, and so on.[4,5] Various ZnO nanostructures including nanowires, nanorods, nanoplates, etc., have been successfully synthesized.[6] In particular, Tusche *et al.*[7] observed the depolarized ZnO (0001) monolayers (MLs) deposited on Ag (111), in which ZnO MLs manifest a planar hexagonal graphitic structure when the thickness is less than four atomic layers. Theoretically, *ab initio* studies[8–12] also revealed that the stability of the planar few ZnO layers (few-ZnOLs) originates from strong in-plane sp^2 hybridized bonds between Zn and O atoms.

In this work, we present a comprehensive investigation on the structure, stability, and bonding characteristic and chemical functionalization of few-ZnOLs via density functional theory (DFT). We find that the formation of stable, planar graphitic structures for few-ZnOLs stems from the strong in-plane covalent-ionic bonding and weak ionic bonding between layers. Most interestingly, fluorination can significantly alter the electronic structure and spin splitting of few-ZnOLs and even give rise to the half metallicity in 2D nanostructures. As the half-metallic materials are semiconducting in one spin channel while metallic in the opposite spin channel, 100% spin-polarized current flow can be generated.[13–17] This may open new application of 2D ZnO nanomaterials in spintronics.

II. COMPUTATIONAL METHOD

Our calculations are performed within the framework of spin-polarized plane-wave DFT, implemented in the Vienna *ab initio* simulation package (VASP).[18] The exchange-correlation potential is approximated by general gradient approximation parametrized by Perdew *et al.*[19] Projected augmented wave[20] method is employed to describe the electron-ion potential. A kinetic energy cutoff of 500 eV is selected for the plane-wave expansion. A $2\times2\times1$ supercell is adopted in structural relaxations [Fig. 1(a)]. Few-ZnOLs are separated by more than 12 Å to avoid artificial interactions between two sheets. The Brillouin zone is sampled by $5\times5\times1$ and $9\times9\times1$ k-point meshes within Monkhorst–

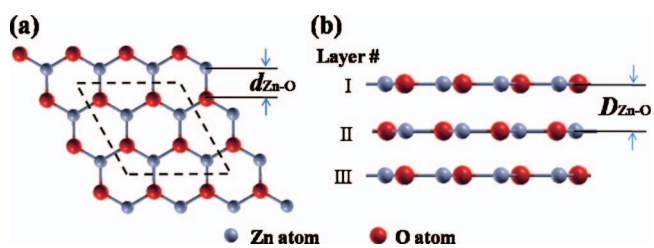

FIG. 1. (a) Top view and (b) side view of a trilayer ZnO sheet, the rhombus plotted in dashed line represents the super cell adopted in the calculations, which contains four unit cells.

[a)]Electronic mail: jlwang@seu.edu.cn.

Pack scheme[21] for geometry optimizations and further calculations on electronic structure and other properties, respectively. All structures are fully relaxed without any symmetry constraint until both the Hellmann–Feynman forces acting on each ion and total energy change are less than 0.005 eV/Å and 1×10^{-4} eV, respectively.

III. RESULTS AND DISCUSSION

A. Pristine few-ZnOLs

Starting from a structure cut from the ZnO wurtzite crystal and terminated with the (0001) polar surface, *ab initio* optimization leads to a planar nonpolar 2D hexagonal honeycomb lattice with D_{3h} symmetry, where Zn (O) atoms of one layer neighboring the O (Zn) atoms of the nearest layer, which is predicted to be the energetically most favorable stacking type for ZnO MLs (Ref. 12) [Figs. 1(a) and 1(b)]. Unlike fourfold coordinated Zn and O atoms in the bulk wurtzite structure, each atom in the planar few-ZnOLs is threefold coordinated, consistent with earlier theoretical predications.[8–12] The calculated intralayer Zn–O bond lengths ($d_{\text{Zn–O}}$) are about 1.91–1.96 Å, while the interlayer distances ($D_{\text{Zn–O}}$) are around 2.37–2.38 Å, in good accord with the earlier computational (1.93 and 2.4 Å) (Ref. 8) and experimental values of 1.91–1.95 and 2.10–2.40 Å,[7] respectively. The excellent agreement suggests that Ag substrate only has a minor effect on the few-ZnOLs, which in turn demonstrates the rationality of neglecting Ag substrate in our computations. It is interesting to note that the intralayer Zn–O bond lengths are shortened a little while the interlayer Zn–O bond lengths are elongated significantly in comparison with the bulk value of 1.98 Å. This shows that the binding nature between interlayer and intralayer Zn–O atoms are very different. The intralayer Zn–O bonds have robust covalent bonding characteristic due to the sp^2 hybridization of Zn and O atoms. Meanwhile, a significant charge transfer from Zn ($\sim0.8e$) to O ($\sim-0.8e$) is also observed, which indicates that ionic interaction also contributes to the intralayer binding. On the contrast, a Zn atom and a corresponding O atom in a neighboring layer form ionic bond through the electrostatic interaction. As the interlayer distances $D_{\text{Zn–O}}$ are relatively large (2.37–2.38 Å), the interaction between the layers is thus relatively weak, which can be clearly seen from the average interlayer binding energy below. This covalent-ionic bonding characteristic can be identified from charge density shown in Fig. 2(a), in which significant charge overlap between intralayer Zn and O atoms can be seen while charge overlap between layers is negligible.

The interlayer interaction can be evaluated by average interlayer binding energy (E_b) per layer of a unit cell defined as

$$E_b = (NE_{\text{ML}} - E_{\text{NLs}})/N, \tag{1}$$

where E_{NLs} is the total energy of the N-layer ZnO sheets in a unit cell, E_{ML} is the energy of the ZnO ML, and N is the number of the layers. As shown in Fig. 2(b), the E_b is less than 0.3 eV per unit cell, indicating that the interaction between neighboring few-ZnOLs is quite weak. Furthermore, the gradually increased interlayer interaction drives the few-ZnOLs go back to wurtzite structure after a critical thickness. Tu and Hu[10] found that a ZnO thin film less than four Zn–O layers prefers the planar graphitic structure rather than the wurtzite structure, in good agreement with the experimental observation.[7] Moreover, when the film goes thicker, it exhibits a wurtzite structure with a nonpolar planar surface.[22,23]

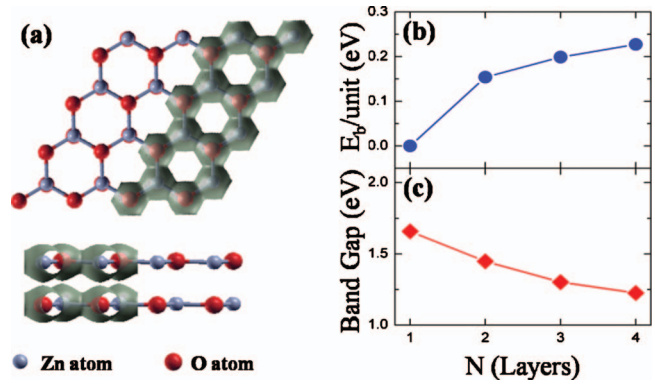

FIG. 2. (a) Top view and side view of calculated total charge density of ZnO bilayer, the isosurface is 0.3 $e/\text{Å}^3$; (b) Average interlayer energy of a unit cell; and (c) band gap as a function of few-ZnOLs thickness.

Regarding of electronic structure, different from semimetal graphene, few-ZnOLs are semiconductor and the band gap smoothly decreases as the thickness increases [see Fig. 2(c)]. Band structures of the mono- and bilayer ZnO sheets (see Fig. 3) indicate that the few-ZnOLs retain the direct band gap property of their wurtzite bulk. The component analysis on the bands of the ZnO ML reveals that the valence bands near the Fermi level are mainly composed of O $2p$ orbitals. Particularly, the two top valence bands in red mainly originated from the p_x and p_y states of oxygen. They are quite delocalized as the intralayer sp^2 hybridization results in a notably strong interaction between O $2p_x$, $2p_y$, and Zn $3d$ orbitals. On the other hand, the O p_z orbitals do not form π-bonding with its neighboring Zn d orbitals and thus are rather localized, unlike the case of graphene of which π and π^* bands cross at the K point of the Brillouin zone. As for the ZnO bilayer, due to the layer-layer interaction, the bands of each layer are not fully degenerated. As a consequence, the redistribution of bands narrows the band gap [Fig. 2(c),

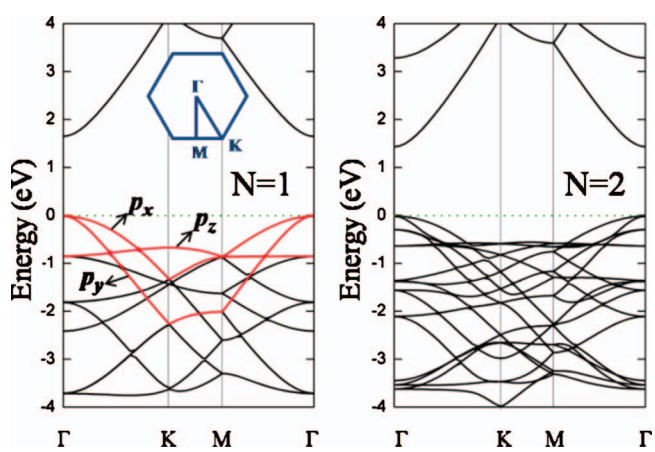

FIG. 3. Calculated band structures of ZnO ML (left panel) and bilayer (right panel). Dotted line refers to the Fermi level. Γ(0,0,0), K(1/3,1/3,0), M(1/2,0,0) refer to special points in the first Brillouin zone.

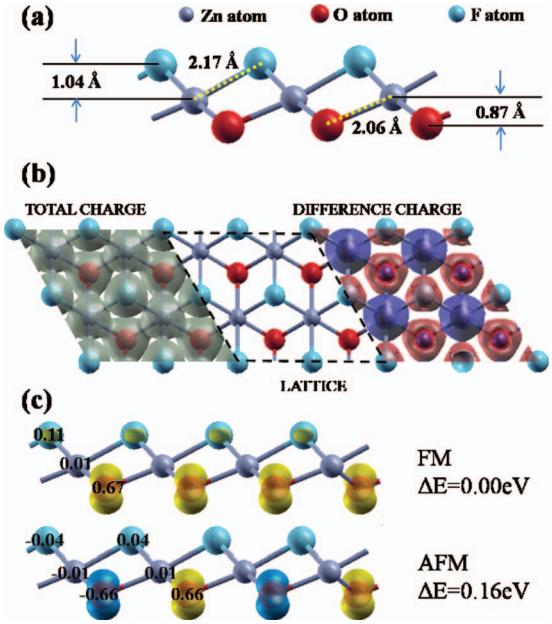

FIG. 4. Optimized structure of F-ZnO ML. (a) Side view with Zn–O and Zn–F bonds labeled by dashed lines. (b) Top view with the rhombus marked in dashed line shows the super cell. Calculated total charge density and charge density difference are shown in the left (0.3 $e/\text{Å}^3$) and right (0.05 $e/\text{Å}^3$) panels, respectively. Positive: red and negative: blue. (c) Spin density of the FM and AFM configurations (0.1 $e/\text{Å}^3$) with their energy difference (ΔE) of super cell given in right. The local magnetic moments are also given.

the right panel of Fig. 3]. Although the systematic underestimation of the band gap is a common drawback of the DFT methods,[24] the dependence of the electronic properties of the few-ZnOLs on their thickness should be valid. This tunable band gap makes few-ZnOLs a good complementary to graphene.

B. Fluorinated few-ZnOLs

On-plane chemical functionalization is a feasible way to modify the electronic and magnetic properties of 2D materials. The fully hydrogenated graphene has been predicted theoretically[25] and synthesized by exposing graphene in hydrogen plasma environment,[26] which turns a semimetal graphene into a semiconductor graphane. Moreover, ferromagnetism in semihydrogenated graphene has been predicted theoretically.[27] Chemical functionalization can also change the indirect gap of the 2D polysilane to a direct gap[28] and the metallic silicon surface to a semiconductor in different cesium coverages.[29] Then, what is the case of 2D few-ZnOLs? Based on the pristine structures above, we study the on-plane fluorinated few-ZnOLs (F-few-ZnOLs). Due to fact that 2D few-ZnOLs are prepared on the Ag (111),[7] we only study one side fluorination of few-ZnOLs here.

We first consider the fluorinated ZnO monolayer (F-ZnO ML). Three different adsorption positions including one hollow site and two top sites (both Zn and O top sites) are taken into account. The energetically most preferred structure is a trilayer configuration with C_{3v} symmetry consisting of a Zn-plane sandwiched between F- and O-planes [Figs. 4(a) and 4(b)]. The distance between these planes are 1.04 and 0.87 Å, respectively. The isosurface of total charge [the left panel of Fig. 4(b)] indicates that each F atom is bonded with the nearest three Zn atoms and the bond length is 2.17 Å. The charge density difference, calculated by subtracting charge density of free Zn, O, and F atoms from that of F-ZnO ML, is displayed in the right panel of Fig. 4(b). Similar to the unfluorinated few-ZnOLs, there is significant charge transfer between Zn atoms and F (O) atoms, corresponding to their covalent-ionic bonding nature. Moreover, the charge transfer between Zn and F atoms weakens the electrostatic interaction between Zn and O atoms. As a result, the $d_{\text{Zn–O}}$ increases to 2.06 Å, i.e., about 8% longer than in the pristine ZnO ML.

In terms of magnetic property, the pristine ZnO ML is nonmagnetic (NM) as each O atom receives enough electrons from the nearest Zn atoms to fill up all p orbitals. However, after fluorination, about one electron transfers from a Zn to a F atom, leaving an electron in O atoms unpaired. Our DFT calculation shows that the F-ZnO ML is a ferromagnetic (FM) coupling with a total magnetic moment of 0.84 μ_B per unit cell and the FM state has lower energy than the NM state by 0.5 eV per unit cell. The spin density [see Fig. 4(c)] indicates that the magnetic moment is mainly located on the O atoms (about 0.67 μ_B per atom), while the F or Zn atoms carry very small spins (less than 0.12 μ_B). This is similar to the situation in ZnO nanoribbons, in which magnetic moments are mainly contributed from edged O atoms.[30–32] We also calculate the antiferromagnetic (AFM) state [see Fig. 4(c)] and found that it is 0.16 eV per supercell higher in energy than the FM state. Using the Heisenberg model and mean field theory, we can get an estimation of the Curie temperature of FM F-ZnO ML of 460 K, showing that the F-ZnO ML is a robust ferromagnet.

The band structure and density of states (DOS) of the F-ZnO ML are presented in Fig. 5. The partial DOS reveals that O $2p$ orbitals are pronounced near the top of valence band [see Fig. 5(b)]. The large spin splitting leads to the states around the Fermi level being wholly contributed from the spin-down states of p states of O atoms and d states of Zn atoms; some O $2p_z$ orbitals are even pushed above the Fermi level [see Fig. 5(a)] leaving the valence states in the spin-up channel about 0.5 eV below the Fermi level. Thus the magnetism is mainly from the O $2p_z$ orbitals in the spin-up channel. The long-range magnetic coupling among these O p moments results in a FM ordering of the F-ZnO ML. Similar magnetic ordering between p moments in 2D network was also observed on partially hydrogenated graphene[27] and Si (111) surfaces.[33] Most importantly, the band structure shows that the spin-down channel is metallic with the O p states crossing the Fermi level, while the spin-up channel is semiconducting with a quite large band gap of about 4.40 eV. In another words, the fluorination leads to a significant electronic structure modification and turns the semiconducting ZnO ML into the half-metallic F-ZnO ML. Moreover, the half-metal gap, defined as the difference between the Fermi level and the topmost occupied spin-up band, is 0.537 eV, which is the largest half-metal gap ever reported. This gap is large enough for high temperature operation up to 1000 K. In order to validate the half-metallic property of F-ZnO, we further exploited the exchange-correlation functional with both the local spin density approximation (LSDA) and the

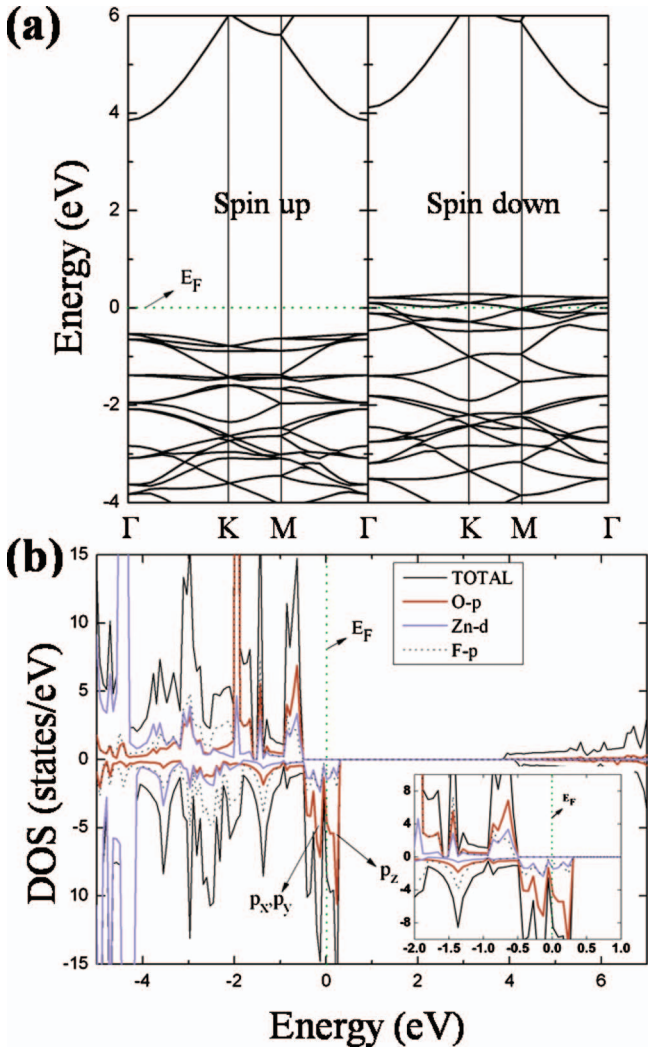

FIG. 5. Calculated band structure (a) and density of state (b) of the F-ZnO ML.

fully localized limit of the LSDA+U method.[34] Here, the on-site *d*-*d* Coulomb interaction, U, and the on-site exchange interaction, J, are 4.5 and 0.5 eV, respectively, which are typical values for the 3*d* transition metals.[35] Both LSDA and LSDA+U calculations show that F-ZnO layer is a good half metal with the half-metal gaps of 0.671 eV and 0.673 eV, respectively. So we conclude that the half metallicity of F-ZnO ML is robust and independent of the calculation method. Half metallicity was also found in partially hydrogenated boron nitride nanoribbons[36] and edge-passivated ZnO nanoribbons.[32] However, as the on-plane chemical modification on 2D sheet does not need to cut the ZnO sheet into ribbon, it is expected to be realized experimentally more easily.

Although the F-ZnO ML shows novel half metallicity with considerable magnetic moment, its fabrication is still a big challenge. Experimentally, synthesis of few-ZnOLs might be easier. Can the F-few-ZnOLs maintain the half metallicity as the thickness increases? How is the stability of F-few-ZnOLs? To answer these questions, we study the fluorination on multilayer ZnO sheet with layer numbers N=2, 3, and 4. Similar to the F-ZnO ML, the fluorination leads to

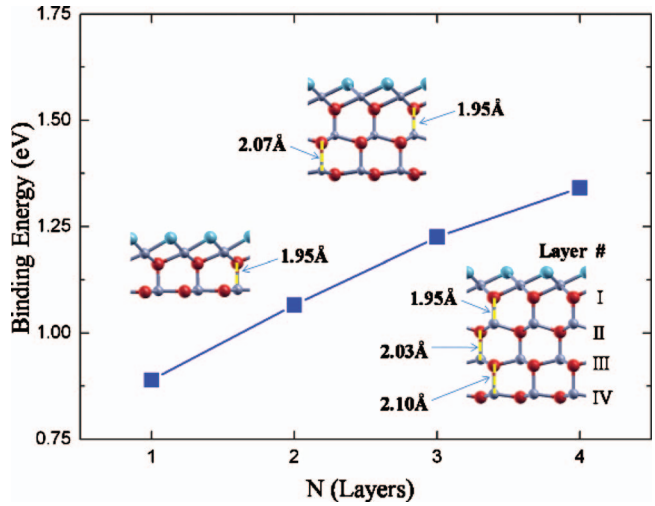

FIG. 6. Binding energy s the thickness of F-few-ZnOLs. The inset shows the optimized structures of the F-few-ZnOLs with N=2–4.

the reduction in the interlayer Zn–O bonds (D_{Zn-O}). Moreover, the farther the layer is from F atoms, the larger the D_{Zn-O} is, e.g., the D_{Zn-O} of the four-layer F-few-ZnOLs are 1.95, 2.03, and 2.10 Å from F side to the other unfluorinated ZnO side, respectively (see the inset in Fig. 6). This means that fluorination turns the original 2D flat ZnO structure to a three-dimensional bulklike one and thus significantly increases the interlayer binding strength.

The F-few-ZnOLs are also FM with the total magnetic moments per unit cell around 0.8 μ_B (Fig. 7). The Zn atoms in layer II can provide electrons to the O atoms in layer I, which reduces the number of unpaired O *p* electrons in layer I. Meanwhile, as the electrons are transferred from layer II to layer I, the O atoms in layer II cannot gain enough electrons from the Zn atoms, thus, leading to part of O *p* electrons in layer II unpaired and producing certain local magnetic moment. In such a way, the local magnetic moments on O atoms are handed on layer by layer as the layer increases.

In terms of electronic properties, our calculation shows

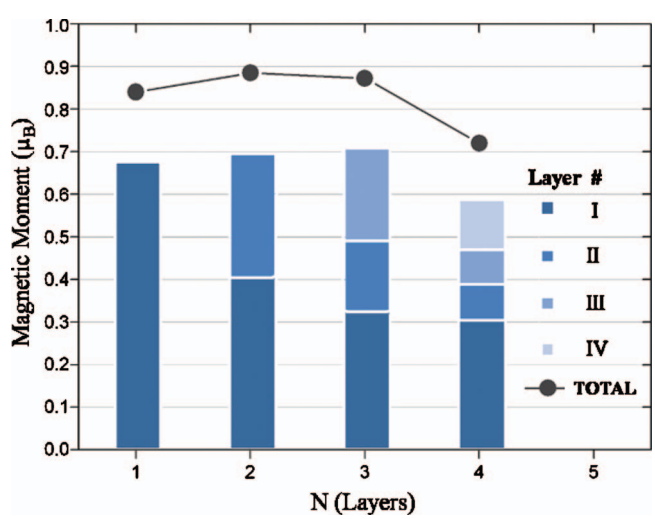

FIG. 7. Total magnetic moments per unit cell vs the thickness of F-few-ZnOLs. The filled bars present the magnetic moments located on O atoms and the different gradation indicates the O atoms in different layers.

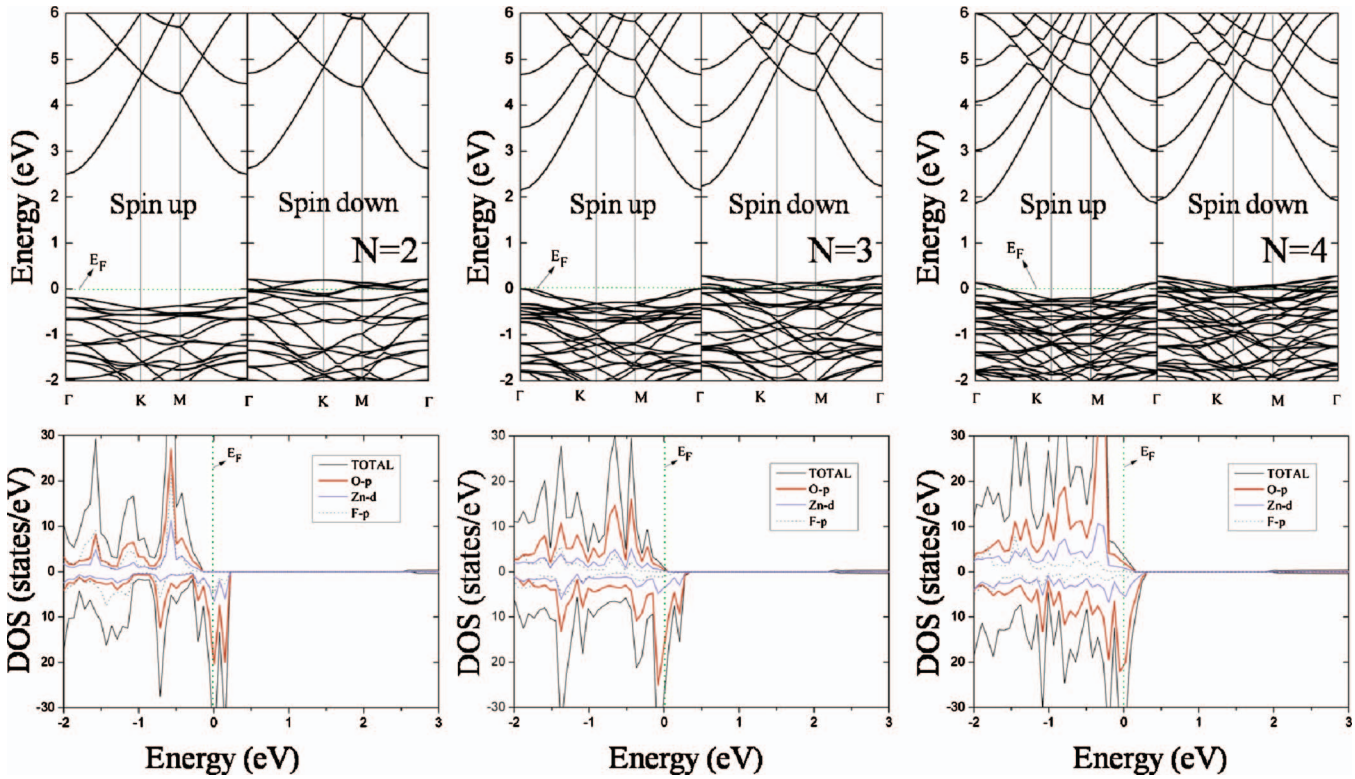

FIG. 8. Calculated band structures and DOS of the fluorinated F-few-ZnOLs with the thickness of N=2, 3, and 4.

that the half metallicity can also be achieved for the F-ZnO bilayer and the half-metal gap is still large enough (0.187 eV) for room-temperature operation. When the thickness is more than three layers, the bands in the spin-up channel begin to cross the Fermi level and the 100% spin polarization is no longer available (see Fig. 8). Nevertheless, for the case of the F-ZnO trilayer, the band only crosses the Fermi level at gamma point by 0.001 eV in the spin-up channel while high spin density crosses the Fermi level in the spin-down channel, which shows that it is actually also a good spin filter and is quasi-half-metal. This trilayer thickness supplies sufficient technical space for experimental realization of few-ZnOLs,[7] and we anticipate that such a half-metallic FM property of the F-few-ZnOLs will give the 2D ZnO based materials great opportunities in future nanodevice industry.

To evaluate the stability of F-few-ZnOLs, the binding energy of F to few-ZnOLs (E_b) is calculated from the formula

$$E_b = E_{ZnO} + (1/2)E_{F_2} - E_{F-ZnO}, \quad (2)$$

where E_{ZnO} and E_{F-ZnO} are the total energy of the pristine and fluorinated few-ZnOLs of a unit cell, and E_{F_2} is the total energy of an F_2 molecule. The calculated binding energy monotonically increases from 0.89 to 1.34 eV with the number of layers varying from 1 to 4 as shown in Fig. 6, which shows that few-ZnOLs can be fluorinated easier than ML.

IV. CONCLUSIONS

We have systematically investigated the structural, electronic, and magnetic properties of the 2D ZnO atomic layers by means of spin-polarized DFT. The pristine few-ZnOLs form stable hexagonal graphitic structures with shortened intralayer Zn–O distances and elongated interlayer Zn–O distance, in good agreement with the experimental observations. Different from the covalent intralayer bonding and van der Waals interlayer interaction in graphene, ours results show that the layered ZnO sheet is attributed to a strong covalent-ionic intralayer bonding and a weak ionic interlayer interaction between Zn and O atoms. The few-ZnOLs are all semiconductor and the band gap decreases with increasing thickness. Furthermore, the on-plane fluorination has been studied in great detail. The fluorination from one side turns the planar few-ZnOLs back to the wurtzitelike corrugated structure and enhances the stability of the 2D ZnO films. The fluorinated few-ZnOLs are found to be FM and the magnetic moments of the F-few-ZnOLs are as high as 0.84, 0.89, 0.87, and 0.72 μ_B per unit cell for N=1–4, respectively. More interestingly, the half-metallicity can be achieved with the thickness less than four layers. The half-metal gap is as large as 0.5 and 0.2 eV for the F-ZnO ML and bilayer, which makes them robust spintronic materials. These diverse electronic and magnetic properties of few-ZnOLs may open new applications of the traditional ZnO materials in nanoelectronics and spintronics. However, due to the limitation of computing capability, here, we have not taken the influence of the substrate into account in this study. How does the substrate affect the electronic structure of the F-few-ZnOLs and whether the half-metallicity can still be preserved need to be further investigated.

ACKNOWLEDGMENTS

This work was supported by the NSF (Grant No. 20873019), the NBRP (Grant Nos. 2010CB923401 and

2009CB623200), the NCET (Grant No. NCET-06-0470), the SRFDP (Grant No. 20090092110025), the NSF of Jiangsu (BK2009264) and the Peiyu Foundations of SEU in China. The authors thank the computational resource at Department of Physics, SEU.

[1] K. S. Novoselov, A. K. Geim, S. V. Morozov, D. Jiang, Y. Zhang, S. V. Dubonos, I. V. Grigorieva, and A. A. Firsov, Science **306**, 666 (2004).
[2] A. H. Castro Neto, F. Guinea, N. M. R. Peres, K. S. Novoselov, and A. K. Geim, Rev. Mod. Phys. **81**, 109 (2009).
[3] L. Y. Zhu, J. L. Wang, T. T. Zhang, L. Ma, C. W. Lim, F. Ding, and X. C. Zeng, Nano Lett. **10**, 494 (2010).
[4] D. C. Look, Mater. Sci. Eng., B **80**, 383 (2001).
[5] Ü. Özgür, Ya. I. Alivov, C. Liu, A. Teke, M. A. Reshchikov, S. Doğan, V. Avrutin, S.-J. Cho, and H. Morkoç, J. Appl. Phys. **98**, 041301 (2005).
[6] L. Schmidt-Mende and J. L. MacManus-Driscoll, Mater. Today **10**, 40 (2007).
[7] C. Tusche, H. L. Meyerheim, and J. Kirschner, Phys. Rev. Lett. **99**, 026102 (2007).
[8] F. Claeyssens, C. L. Freeman, N. L. Allan, Y. Sun, M. N. R. Ashfold, and J. H. Harding, J. Mater. Chem. **15**, 139 (2005).
[9] C. L. Freeman, F. Claeyssens, N. L. Allan, and J. H. Harding, Phys. Rev. Lett. **96**, 066102 (2006).
[10] Z. C. Tu and X. Hu, Phys. Rev. B **74**, 035434 (2006).
[11] R. G. S. Pala and H. Metiu, J. Phys. Chem. C **111**, 12715 (2007).
[12] M. Topsakal, S. Cahangirov, E. Bekaroglu, and S. Ciraci, Phys. Rev. B **80**, 235119 (2009).
[13] Y. W. Son, M. L. Cohen, and S. G. Louie, Nature (London) **444**, 347 (2006).
[14] M. C. Qian, C. Y. Fong, K. Liu, W. E. Pickett, J. E. Pask, and L. H. Yang, Phys. Rev. Lett. **96**, 027211 (2006).
[15] E. Kan, X. Wu, Z. Li, X. C. Zeng, J. Yang, and J. G. Hou, J. Chem. Phys. **129**, 084712 (2008).
[16] L. Zhu and J. Wang, J. Phys. Chem. C **113**, 8767 (2009).
[17] S. Dutta, A. K. Manna, and S. K. Pati, Phys. Rev. Lett. **102**, 096601 (2009).
[18] G. Kresse and J. Furthmuller, Phys. Rev. B **54**, 11169 (1996).
[19] J. P. Perdew, K. Burke, and M. Ernzerhof, Phys. Rev. Lett. **77**, 3865 (1996).
[20] P. E. Blöhl, Phys. Rev. B **50**, 17953 (1994).
[21] H. J. Monkhorst and J. D. Pack, Phys. Rev. B **13**, 5188 (1976).
[22] B. Meyer and D. Marx, Phys. Rev. B **67**, 035403 (2003).
[23] G. Kresse, O. Dulub, and U. Diebold, Phys. Rev. B **68**, 245409 (2003).
[24] J. Paier, R. Hirschl, M. Marsman, and G. Kresse, J. Chem. Phys. **122**, 234102 (2005).
[25] J. O. Sofo, A. S. Chaudhari, and G. D. Barber, Phys. Rev. B **75**, 153401 (2007).
[26] D. C. Elias, R. R. Nair, T. M. G. Mohiuddin, S. V. Morozov, P. Blake, M. P. Halsall, A. C. Ferrari, D. W. Boukhvalov, M. I. Katsnelson, A. K. Geim, and K. S. Novoselov, Science **323**, 610 (2009).
[27] J. Zhou, Q. Wang, Q. Sun, X. S. Chen, Y. Kawazoe, and P. Jena, Nano Lett. **9**, 3867 (2009).
[28] N. Lu, Z. Li, and J. Yang, J. Phys. Chem. C **113**, 16741 (2009).
[29] H. Y. Xiao, X. T. Zu, Y. F. Zhang, and L. Yang, J. Chem. Phys. **122**, 174704 (2005).
[30] A. R. Botello-Méndez, F. López-Urías, M. Terrones, and H. Terrones, Nano Lett. **8**, 1562 (2008).
[31] A. R. Botello-Méndez, F. López-Urías, M. Terrones, and H. Terrones, Nano Res. **1**, 420 (2008).
[32] Q. Chen, L. Y. Zhu, and J. L. Wang, Appl. Phys. Lett. **95**, 133116 (2009).
[33] S. Okada, K. Shiraishi, and A. Oshiyama, Phys. Rev. Lett. **90**, 026803 (2003).
[34] V. Anisimov, F. Aryasetiawan, and A. Lichtenstein, J. Phys.: Condens. Matter **9**, 767 (1997).
[35] P. Gopal and N. A. Spaldin, Phys. Rev. B **74**, 094418 (2006).
[36] W. Chen, Y. Li, G. Yu, C. Z. Li, S. B. Zhang, Z. Zhou, and Z. Chen, J. Am. Chem. Soc. **132**, 1699 (2010).